Materials Today Bio 31 (2025) 101517

Contents lists available at ScienceDirect

Materials Today Bio

journal homepage: www.journals.elsevier.com/materials-today-bio

Supramolecular peptide hydrogel epitope vaccine functionalized with CAR-T cells for the treatment of solid tumors

Pengxiang Yang [a,b,*,1], Xiaomin Yao [a,1], Xue Tian [c], Yuehan Wang [d], Leilei Gong [a,b,**], Yumin Yang [a,b,***], Jing Jie [c,****]

[a] Key Laboratory of Neuroregeneration of Jiangsu Province and Ministry of Education, Co-Innovation Center of Neuroregeneration, NMPA Key Laboratory for Research and Evaluation of Tissue Engineering Technology Products, Nantong University, 226001, Nantong, PR China
[b] Engineering Research Center of Integration and Application of Digital Learning Technology, Ministry of Education, 100034, Beijing, PR China
[c] Department of Clinical Laboratory, The Second Affiliated Hospital of Nantong University, 226001, Nantong, PR China
[d] Medical School of Nantong University, Nantong University, 226001, Nantong, PR China

ARTICLE INFO

Keywords:
Supramolecular peptide hydrogel
Epitope vaccine
CAR-T cells
Active and passive immune responses
Memory cells

ABSTRACT

Chimeric antigen receptor T-cell (CAR-T) therapy, which benefits from the perfect combination of gene editing techniques and antibody engineering, has shown outstanding clinical efficacy in hematological malignancies. Solid tumors present the next challenge due to their extremely complicated microenvironment and structural characteristics. Targeting efficiency and persistence are currently bottleneck issues in the clinical treatment of CAR-T. Beyond drugs and cytokines, biomaterials can modulate the immune response, assisting adoptive CAR-T cells in exerting their function. In this study, a supramolecular peptide hydrogel epitope vaccine was designed to serve as both a preparation medium and a reservoir for CAR-T cells. The self-assembling peptide formed a nanofiber scaffold through non-covalent interactions of amphiphilic amino acids and ion stabilizers. Firstly, the complementary peptide conjugated vaccine epitopes and CAR-T target sites were derived from different extracellular domains of the HER2 protein, and the combination treatment improved tumor antigen spreading and targeting efficiency. The epitope hydrogel promoted CAR-T cell proliferation, cytotoxic activity, and lymphocyte subpopulation transformation. Furthermore, the supramolecular peptide epitope vaccine encapsulated CAR-T (SPEV-CAR-T) induced endogenous humoral and cellular immune responses through a sustained release of the hydrogel and CAR-T cells, demonstrating superior anti-tumor effects in an in vivo mouse model. Most importantly, SPEV-CAR-T induced central memory cells in systemic immune tissues, addressing the poor persistence of single CAR-T therapy. The integration and complementation of active and passive immune responses in this all-in-one hydrogel epitope vaccine and CAR-T system facilitated a sequential succession of endogenous and exogenous immune responses, promoting persistent and specific tumor attack. SPEV-CAR-T showed superior therapeutic effects in solid tumors.

1. Introduction

Immunotherapy has undergone rapid development in the last twenty years, revolutionizing the treatment of various diseases. Clinical drugs and preparations have been exquisitely designed based on a deep understanding of the immune system [1]. Chimeric antigen receptor T-cell

* Corresponding author. Key Laboratory of Neuroregeneration of Jiangsu Province and Ministry of Education, Co-Innovation Center of Neuroregeneration, NMPA Key Laboratory for Research and Evaluation of Tissue Engineering Technology Products, Nantong University, 226001, Nantong, PR China.
** Corresponding author. Key Laboratory of Neuroregeneration of Jiangsu Province and Ministry of Education, Co-Innovation Center of Neuroregeneration, NMPA Key Laboratory for Research and Evaluation of Tissue Engineering Technology Products, Nantong University, 226001, Nantong, PR China.
*** Corresponding author. Key Laboratory of Neuroregeneration of Jiangsu Province and Ministry of Education, Co-Innovation Center of Neuroregeneration, NMPA Key Laboratory for Research and Evaluation of Tissue Engineering Technology Products, Nantong University, 226001, Nantong, PR China.
**** Corresponding author. Department of Clinical Laboratory, The Second Affiliated Hospital of Nantong University, 226001, Nantong, PR China.
E-mail addresses: yangpengxiang@ntu.edu.cn, yangpengxiang@163.com (P. Yang), 105799988@qq.com (L. Gong), yangym@ntu.edu.cn (Y. Yang), jiejing1103@126.com (J. Jie).
[1] These authors contributed equally.

https://doi.org/10.1016/j.mtbio.2025.101517
Received 2 August 2024; Received in revised form 3 January 2025; Accepted 21 January 2025
Available online 22 January 2025

(CAR-T) therapy, which benefits from the combination of gene editing techniques and antibody engineering, holds great promise as an advanced and personalized cancer treatment [2,3]. It has shown significant success in treating hematological malignancies, but solid tumors present the next challenge due to their complex microenvironment and structural characteristics [4,5]. Numerous clinical and preclinical efforts, including cytokines, molecular inhibitors, immune checkpoint blockade, vaccination, and adoptive cell transfer, have been made to overcome these obstacles [6,7]. However, the current clinical outcomes of CAR-T treatments are unsatisfactory, as they are effective for only a small number of patients due to poor persistence or inefficacy of the synergistic effects [8].

The recognition and clearance of tumor cells by CAR-T cells depend on the targeted CAR molecule. Target selection is a critical determinant, and off-target effects may potentially lead to adverse effects, toxicity, and unintended target disruption [9]. The affinity of single-chain variable fragments (scFv) is unstable due to tumor antigen modulation and the microenvironment [10]. Combining targeted therapies, involving the same or different molecules, has become a consensus in clinical strategies [11]. Multiple studies focus on the joint application of antibodies or immune checkpoint inhibitors with CAR-T cells to enhance targeting. While these reagent combinations can kill tumor cells, they often fail to achieve persistent immune attacks due to exacerbated systemic inflammatory responses leading to cytokine release syndrome, which is burdensome for patients [4,12]. Active immunotherapy works with the body's immune system to induce long-lasting tumor immune attacks.

Vaccination, an active immunization method, aims to generate permanent immunological memory against both infectious and non-infectious diseases, making a tremendous contribution to human medicine and health. In the past century, over one hundred vaccines have been licensed for clinical use, including therapeutic and preventive vaccines [13,14]. Cancer vaccines deliver tumor-associated antigens in various formulations, such as live-attenuated, inactivated, toxoid, protein subunit/conjugate, or nucleic acid [15]. Vaccine components are taken up by antigen-presenting cells (APCs) and transported to local draining lymph nodes (LNs), where B and T cells detect the antigen and initiate the adaptive immune response. Immune cells mobilized from the host's immune system attack tumors by sensing the systemic microenvironment [16]. Designed amphiphile-ligand vaccines traffic to lymph nodes and decorate the surfaces of antigen-presenting cells, thereby priming CAR-T cells [17]. Additionally, RNA vaccines drive the expansion and efficacy of claudin-CAR-T cells against solid tumors [18]. CAR-T treatment assisted by vaccines has the potential to radically eliminate tumors; however, research in this field is still in its early stages, and the mechanisms of the synergistic effects and integrative studies remain unresolved.

With advances in the analysis of pathogen antigen structures, subunit vaccines containing only antigenic proteins or epitopes address the limitations of traditional vaccines. However, their reduced immunogenicity necessitates the co-administration of adjuvants to elicit immune responses sufficient for memory formation [19]. Adjuvants are chosen for their ability to non-specifically enhance both cellular and humoral immune responses, including aluminum hydroxide and oil/water-based adjuvants [20]. As the knowledge of immunology expands, a major goal of the cross-disciplinary field of immunoengineering is to exert spatial and temporal control over the immune system's activity. This is primarily achieved by using rationally designed biomaterials to produce efficient and safe vaccine adjuvants and to shed light on their less-understood functions [21,22].

Supramolecular chemistry involves chemical systems formed by the self-assembly of molecular subunits via non-covalent interactions [21,23]. Peptide delivery systems have been developed to create novel peptide vaccines aimed at modulating the adaptive immune response and enhancing the immunogenicity of antigenic epitopes [24]. Previous research has begun to redefine vaccine development by emphasizing how physical parameters such as size, shape, charge, and other material properties can alter the immune response [25]. We developed a supramolecular peptide vaccine self-assembled from synthetic amphiphilic peptides conjugated with $CD8^+$ T-cell epitopes (TRP2). This novel vaccine effectively stimulated the maturation of dendritic cells (DCs) and augmented the therapeutic antitumor effect in vivo against melanoma, outperforming peptide vaccines formulated in nano-emulsions and adjuvanted with CpG [24].

Here, we designed and generated a smart supramolecular peptide hydrogel epitope vaccine, which self-assembles driven by non-covalent interactions of amphiphilic amino acids and calcium/magnesium ion stabilizers. The hydrogel epitope vaccine was used as both a preparation medium and a reservoir for CAR-T cells. The conjugated epitope sequence E75 was derived from human epidermal growth factor receptor 2 (HER2), a validated therapeutic target for breast and gastric cancers. This epitope hydrogel promoted CAR-T cell proliferation, cytotoxic activity, and lymphocyte subpopulation transformation. Vaccine epitopes and CAR-T target sites are from different extracellular domains of the HER2 protein, and the combination treatment improved tumor antigen spreading and targeting efficiency. Furthermore, the supramolecular peptide epitope vaccine encapsulated CAR-T (SPEV-CAR-T) induced endogenous humoral and cellular immune responses through a sustained release of the hydrogel and CAR-T cells, demonstrating superior anti-tumor effects in an in vivo mouse model. Most importantly, SPEV-CAR-T induced central memory cells in systemic immune tissues, addressing the poor persistence of single CAR-T therapy. The integration and complementation of active and passive immune responses in this all-in-one hydrogel epitope vaccine and CAR-T system facilitated a sequential succession of endogenous and exogenous immune responses, promoting persistent and specific tumor attacks. SPEV-CAR-T showed superior therapeutic effects in solid tumors (Fig. 1).

2. Materials and methods

2.1. Reagents and antibodies

The self-assembling peptides KFKFEFEF (molecular weight: 1120.70 Da) and KFKFEFEFGGEKIFGSLAFL (molecular weight: 2383.05 Da) were commercially synthesized by Bankpeptide Biological Technology Co., Ltd. (Hefei, China). Fluorochrome-labeled anti-human monoclonal antibodies (CD3, CD4, CD8, CD25, CD45RA, CD69, CD80, CD86, CD62L, IFN-γ, MHC I, PD-1) were purchased from eBioscience (San Diego, CA). CD3/CD28 Dynabeads were purchased from Miltenyi Biotec (San Diego, CA). IL-15 was procured from PeproTech (London, UK). The LDH release assay kit was purchased from Promega Corporation (Madison, WI, USA). The Proteome Profiler Cytokine Array kit was obtained from R&D Systems (Minnesota, USA). ELISA kits were purchased from eBioscience (San Diego, CA). CCK-8 solution was purchased from Kumamoto (Japan).

2.2. Cell lines and animals

Experimental animals, including 6-8 week-old NSG mice and C57BL/6 mice, were purchased from Beijing biocytogen and Beijing Vital River Laboratory. Humanized mice were generated from $CD34^+$ umbilical cord blood-derived hematopoietic stem cells (HSCs, HLA-$A2^+$). All animal experiments adhered to the animal healthcare regulations of the Ethics Committee of Nantong University, China (Accession No. S20220220-009). Human SKBR3 and MDA-MB231 cells were obtained from the Chinese Academy of Sciences. HER2-CAR-T cells were generated as previously described [4,26]. To ensure the accuracy of immune responses, the DCs and T cells used in the experiments were derived from peripheral blood mononuclear cells (PBMCs) of HLA-$A2^+$ donors from The First People's Hospital of Nantong (Accession No. 2022KT030). Monocytes were isolated using EasySep enrichment kits (STEMCELL Technologies), and after purification, immature DCs were

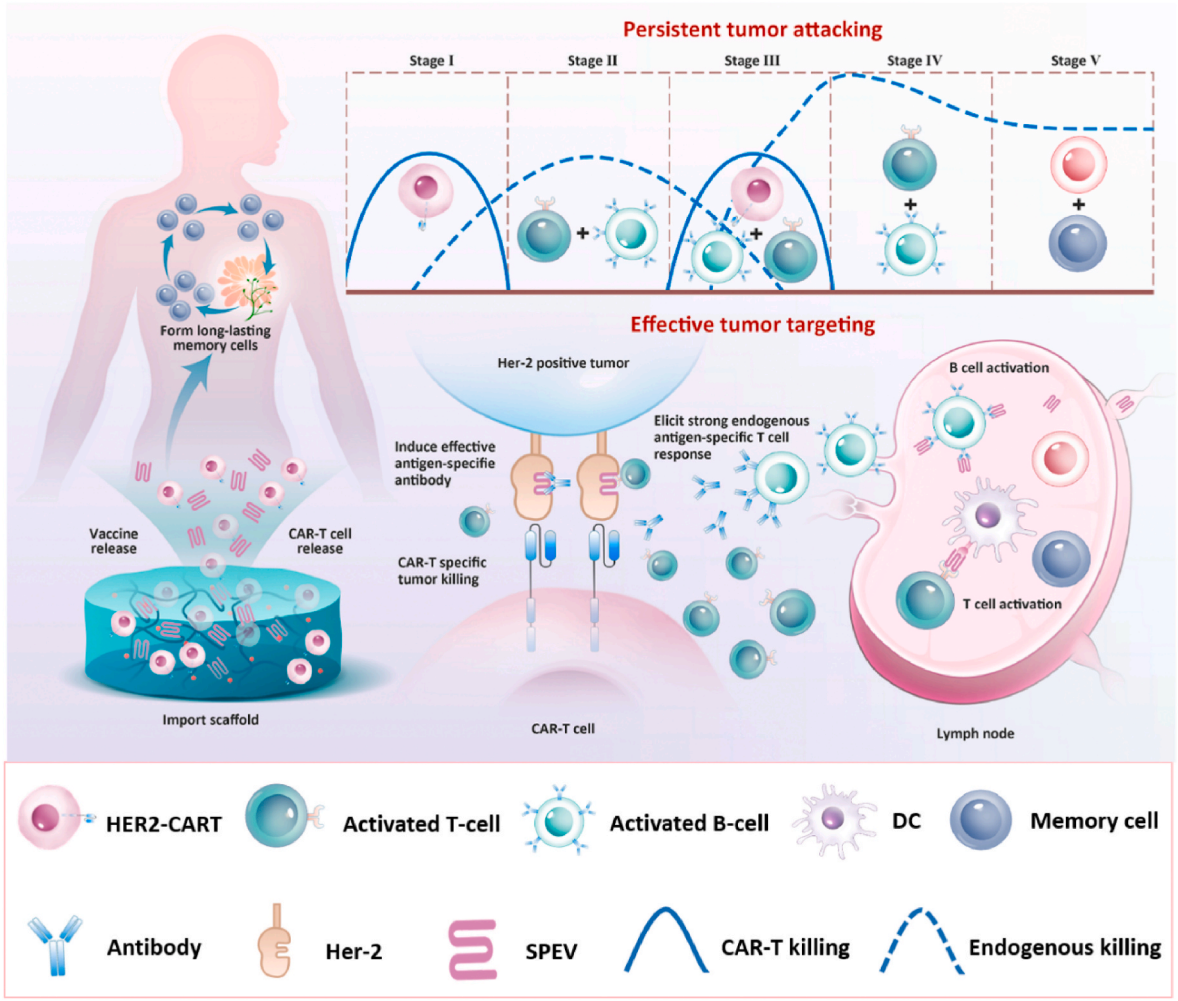

Fig. 1. Supramolecular peptide hydrogel epitope vaccine functionalized with CAR-T cells for the treatment of solid tumors. Left: Schematic illustration of anti-tumor effects of SPEV-CAR-T in body. Upper right: The persistent tumor attacking includes 5 stages. Stage I: First injection of CAR-T killing; Stage II: First injection of SPEV activated T-cell and B-cell killing; Stage III: Second injection of CAR-T killing combined with SPEV activated T-cell and B-cell killing; Stage IV: Second injection of SPEV activated T-cell and B-cell killing; Stage V: Immune memory cells. The solid line represents the killing induced by injection of CAR-T, while the dashed line represents the endogenous killing induced by SPEV-CAR-T. Bottom right: Combined targeting of SPEV-CAR-T. Firstly, HER-2 targeted killing of CAR-T; Secondly, targeted killing induced by activated T/B cells. The E75 epitope and CAR-T target sites are from different extracellular domains of the HER2. This all-in-one hydrogel epitopes vaccine and CAR-T system integrates and complements active and passive immune responses. The sequential activation of endogenous and exogenous immune responses promotes persistent and specific tumor attacks, demonstrating superior therapeutic effects in solid tumors.

induced by adding IL-4 (20 ng/mL) and GM-CSF (100 ng/mL). Cells were cultured in RPMI-1640 medium with 10 % FBS.

2.3. Preparation and characterization of E75 epitope vaccine hydrogel

The self-assembling peptide KFKFEFEF was conjugated to the hydrophilic E75 epitope sequence KIFGSLAFL to form the supramolecular peptide epitope vaccine (FEFK-E75). It was prepared by solid-phase synthesis and characterized by HPLC and MS. FEFK-E75 formed a hydrogel at a concentration of 50 mg/mL. Fiber aggregation or bundles were observed after adding Ca^{2+}/Mg^{2+} ion stabilizers at a concentration of 1 mg/mL. The microstructure of the hydrogel was observed under a Transmission Electron Microscope (TEM). The secondary structure of the polypeptide was analyzed by circular dichroism (CD). The elastic modulus and loss modulus of FEFK-E75 were analyzed by rheology to evaluate whether it was in a hydrogel state.

2.4. Cell viability

T cells were cultured in a medium containing FEFK-E75 hydrogel for 24 h and then washed three times with PBS after the supernatant was discarded. Cell viability was evaluated through dead and live staining. Working solutions containing LiveDye and NucleiDye were added. After culturing for another 30 min, cell viability was analyzed by flow cytometry.

2.5. Cell proliferation

CAR-T cells were used to illustrate the effect of the hydrogel on cell proliferation. CAR-T cells were added to a 96-well plate at a density of 3000 cells per well. After culturing in medium or FEFK-E75 for 48 h, 10 μL of CCK-8 solution was added and cultured for 2 h. Then, OD 450 nm was measured using a microplate reader.

$CD8^+$ T cells were used to illustrate the effect of the hydrogel on the proliferation of endogenous lymphocytes. First, DCs were cultured in medium, FEFK-E75, CAR-T, or SPEV-CAR-T for 48 h. CFSE-labeled $CD8^+$T cells were added and co-cultured for 72 h. The proliferation of T cells was evaluated by detecting the CFSE fluorescence intensity of $CD8^+$T cells using flow cytometry. CFSE-positive $CD8^+$T cells were sorted and placed in the aforementioned four microenvironments at

different effector-to-target ratios. These cells were then co-cultured with HER2-positive target cells, and their cytotoxic activity was assessed after 4 h.

2.6. Flow cytometry analysis

To analyze DC uptake, FITC-labeled E75 peptide and FEFK-E75 were added to the DC culture medium, respectively. Cells were collected 6 h later and analyzed by flow cytometry. To separate cells from the peptide hydrogel by alternating use of 0.5 mg/mL collagenase and low-concentration 0.05 % trypsin. During enzymatic digestion, the cell status was monitored under a microscope to prevent prolonged digestion that could lead to cell damage, minimizing the exposure time of cells to the enzymes. Gentle mechanical pipetting or low-speed centrifugation was employed to assist in cell separation during hydrogel degradation, avoiding excessive handling. After enzymatic degradation with trypsin or collagenase, the enzyme activity was neutralized with serum-containing medium, and cells were collected by low-speed centrifugation (300 g, 5 min). The cells were washed 2–3 times with PBS to thoroughly remove enzyme residues. Mean fluorescence intensity (MFI) and the percentage of FITC-positive cells were recorded. Fluorescence intensity (FI) was calculated using the formula: FI = MFI × positive percentage.

To study the induction of DC maturation by the hydrogel epitope vaccine in vitro, DCs were separated and cultured from human blood as previously described. Cells were placed in wells at a density of 1×10^6/mL. Two groups of stimuli were used: E75 (20 μg/mL) and FEFK-E75. The E75 concentration remained consistent among groups. After 24 h, cells were collected, and CD86 and MHC I fluorescent antibodies were added and incubated for another half hour before being detected by flow cytometry.

In the mouse prophylactic model, the spleen was collected, and lymphocytes were isolated 4 days after tumor bearing. Cell phenotype and activation status were analyzed by flow cytometry. The antibodies used for staining included human CD45RA, CD62L, CD69, CD25, and PD-1.

In the mouse breast cancer therapeutic model, the tumor tissues were harvested 28 days after tumor grafting. Tumor-infiltrating lymphocytes were isolated and stained with fluorescent antibodies for CD3, CD4, CD8, and IFN-γ. The proportions of $CD4^+IFN\text{-}\gamma^+$ and $CD8^+IFN\text{-}\gamma^+$ cell subpopulations were analyzed by flow cytometry.

To study DC maturation in vivo, lymph nodes of mice were harvested 7 days after the last immunization in the mouse anti-breast cancer therapeutic model. After grinding, mononuclear cells were obtained and stained with fluorescent antibodies for CD11c, CD80, and CD86, then analyzed by flow cytometry.

2.7. ELISA

The supernatant from DCs stimulated with different stimuli was collected after 24 h. The levels of IFN-γ, TNF-α, and IL-1β were detected by sandwich ELISA according to the manufacturer's instructions. Ten days after the first immunization or seven days after the second immunization, orbital blood from the immunized mice was collected. Sera were obtained from the blood. E75-specific antibodies IgG, IgG1, and IgG2c in plasma were determined using ELISA as previously described.

2.8. Therapeutic and prophylactic models of breast cancer

In the therapeutic model, humanized NSG-mice were subcutaneously injected with 5×10^5 SKBR3 cells under the breast. Seven days after tumor challenge, mice were randomly divided into four groups (N = 4 per group) and treated with the following agents: PBS, FEFK-E75, CAR-T, and SPEV-CAR-T. CAR-T was injected through the tail vein, while the other groups were injected subcutaneously into the groin. Two vaccine injections were given at a 14-day interval. The dose of CAR-T was 5×10^6 cells/mouse, and FEFK-E75 was 50 μg/mL. Tumor weight and volume were monitored daily. Eye blood was collected ten days after the first immunization and seven days after the second immunization. Serum was separated from the blood and used for antibody titer detection. Three days after each immunization, mouse spleens were ground, and mononuclear cells were isolated for further cultivation to detect splenic proliferation, cytotoxicity, cytokines, and T cell subpopulations.

In the prophylactic model, mice were grouped as described above. One week after the final immunization, a tumor challenge of 5×10^5 SKBR3 cells was performed subcutaneously. The tumor volume was monitored every two days.

2.9. CAR-T release and homing efficiency study

To assess the effect of hydrogels on CAR-T release, CAR-T cells were labeled with luciferase (Luc). C57BL/6 mice were injected with Luc-labeled CAR-T or SPEV-CAR-T subcutaneously and observed under the Xenogen IVIS imaging system on days 1, 3, 5, and 7 (N = 3 per group).

For evaluating the homing efficiency of CAR-T, humanized NSG-mice were first challenged with 1×10^6 SKBR3 cells. Seven days later, mice were divided into two groups (N = 4 per group). Luc-labeled CAR-T or SPEV-CAR-T were injected into the mice, respectively. Tumors were collected every two days. Tumor-infiltrating lymphocytes were obtained by Ficoll and detected by flow cytometry.

2.10. Proteome profiler array

Orbital blood sera from immunized mice in the therapeutic model were obtained. Cytokine levels were determined according to the Proteome Profiler Array instructions. Briefly, the membrane was first immersed in blocking solution for 1 h. The sample was added and incubated overnight. Detection antibodies, streptavidin, and Chemi Reagent Mix were added successively, and finally exposed for detection.

2.11. LDH release assay

The LDH release kit was used to measure the effects of different culture environments on CAR-T cell cytotoxicity. SKBR3 cells in the logarithmic growth phase were used as target cells and co-cultured with effector cells at effector-to-target ratios of 6.25:1, 12.5:1, and 25:1. After 4 h, the supernatant was harvested and placed in a new culture plate, with the addition of substrate solution. After 30 min, the termination solution was added. OD 450 nm was measured using a microplate reader, and the concentration of LDH was calculated using a standard curve. The percentage of specific killing was calculated as follows: Specific killing (%) = [(Experimental release - Spontaneous release)/(Total release - Spontaneous release)] × 100 %.

2.12. Affinity of CAR-T

HER2 protein was synthesized and labeled with FITC. CAR-T cells were inoculated into a 96-well plate at 1×10^5 cells/well. FITC-HER2 protein was diluted in multiple ratios and added to each well. After 24 h, the cells were collected and washed with PBS to remove the unbound protein. Cells were re-suspended in PBS, and CAR-T cells bound to HER2 protein were detected by flow cytometry. The binding curve was plotted with protein concentration as the horizontal coordinate and MFI as the vertical coordinate.

2.13. Statistical analysis

All data were expressed as mean ± S.D. Statistical analyses were performed using GraphPad Prism 8.0. Differences between two groups were compared using Student's t-test. Two-way ANOVA was applied for comparisons among multiple groups. The experiment repeated at least three times. The threshold for statistical significance was $P < 0.05$.

3. Results

3.1. Preparation and characterization of supramolecular peptide hydrogel epitope vaccine

The supramolecular peptide hydrogel epitope vaccine was synthesized using solid-phase synthesis by linking the self-assembling peptide KFKFEFEF with the hydrophilic E75 epitope sequence KIFGSLAFL (designated as FEFK-E75). The HPLC and MS spectra of FEFK-E75 are shown in Supplementary Figs. 1–2. E75 is a nine-amino acid MHC class I peptide derived from the extracellular HER2 protein (amino acids 369–377), which is highly expressed in multiple cancer types (Fig. 2A). The supramolecular peptide developed into long fibers within 30 min, and the formation of fiber aggregation or bundles was observed upon the addition of Ca^{2+}/Mg^{2+} ion stabilizers. The length of these nanofibers increased with assembly time, forming more extensive nanofibrous networks via an end-to-end fiber-fiber aggregation mechanism. The TEM images showed that nanofibers were either singly distributed or aggregated through entanglements (Fig. 2B). Circular dichroism results indicated a typical β-sheet spiral secondary structure composition, with a peak at 197 nm and troughs at 204 nm and 219 nm (Fig. 2C). Rheological analysis showed that the elastic modulus was greater than the loss modulus, confirming that FEFK-E75 formed a hydrogel state. Peptide hydrogels, due to their good biocompatibility, are preferred carriers for delivering cells or drugs. CAR-T cells were encapsulated into the nanofiber epitope vaccine by gently mixing the hydrogel with the cell suspension. Fig. 2D and E demonstrate that the encapsulation of cells did not significantly alter the hydrogel modulus.

CAR-T lymphocytes cultured with FEFK-E75 epitope vaccine hydrogel showed high cell viability and functionality. As shown in Fig. 2F and G, more than 90 % of cells remained viable, with no significant differences observed over the first 7 days, indicating good compatibility. The epitope peptides in the hydrogel, compared to naked peptides, provided superior stability and high immunogenicity, and were better recognized by antigen-presenting cells. We compared the uptake of the E75 peptide and the FEFK-E75 epitope vaccine by dendritic cell (DC). The results indicated that FEFK-E75 significantly enhanced antigen uptake compared to the individual epitope peptide (Fig. 2H and I). Flow cytometry analysis revealed that FEFK-E75 significantly promoted the expression of CD86 (28.0 %) and MHC I (38.4 %), markers of DC maturation (Fig. 2J, Supplementary Fig. 3). After 48 h of cell culture, cytokine detection in the supernatant showed that DC induced by the hydrogel epitope vaccine secreted higher levels of TNF-α and IL-1β (Fig. 2K, Supplementary Fig. 4). These results suggest that the peptide hydrogel epitope vaccine significantly enhances DC uptake and maturation, demonstrating better immunogenicity compared to the naked epitope.

3.2. Peptide hydrogel epitope vaccine promoted CAR-T cells proliferation and subpopulation transformation

The number and status of CAR-T cells are essential for sustained antitumor effects. Therefore, we first investigated the effect of hydrogel as a delivery carrier on the functional status of CAR-T cells. Fig. 3A shows the position of CAR-T target sites and E75 epitope peptides in the extracellular segment of HER2, demonstrating that CAR-T does not bind to E75. Affinity tests further confirmed that the epitope peptide vaccine did not affect the binding of CAR-T cells to target cells, with the affinity constant remaining unchanged regardless of whether the CAR-T cells were encapsulated in the peptide hydrogel epitope vaccine or not (Fig. 3B). The self-assembled peptide epitope hydrogel scaffold provides a three-dimensional cell culture environment. CAR-T cells maintained a high loading efficiency in the peptide hydrogel (Supplementary Fig. 5). To further verify its effect on the functional state of cells, CAR-T cells were cultured in three-dimensional epitope hydrogel and traditional two-dimensional medium environments for 48 h or 168 h. Compared to the traditional culture method, the three-dimensional environment significantly promoted CAR-T cell proliferation, as detected by CCK8 (Supplementary Figs. 6–7).

To evaluate the anti-tumor activity in different culture microenvironments, CAR-T cells were co-incubated with the breast cancer cell line SKBR3. The results demonstrated that the killing rate of CAR-T cells increased with different effector-target ratios, and the group with CAR-T cells encapsulated in the supramolecular peptide epitope vaccine (SPEV-CAR-T) showed a higher killing rate than the single CAR-T group (Fig. 3C, Supplementary Fig. 8). The secretion of IFN-γ and TNF-α was measured by ELISA, revealing that the SPEV-CAR-T group secreted higher levels of these effector cytokines, which positively correlated with the effector-target ratio (Fig. 3D and E). The killing potential of CAR-T cells depends on multiple factors. In addition to cell proliferation assisting CAR-T cytotoxicity, cytokines may affect the distribution of lymphocyte subpopulations through autocrine and paracrine mechanisms. We next investigated cell phenotypes after the long-term culture of CAR-T cells in peptide hydrogel epitope vaccines. The results showed that the proportion of $CD8^+$ T cells did not change significantly, while $CD4^+$ T cells significantly increased in the SPEV-CAR-T group (Fig. 3F and G). Further studies suggested that epitope vaccines maintained higher percentages of central memory cells and naive cells (Fig. 3H and I). Long-term exposure of CAR-T cells to tumor antigens may lead to cell phenotype shifting from functional to an exhausted type. To further investigate the functional activation status, we analyzed the expression level of surface PD-1 on CAR-T cells by flow cytometry. The exhaustion marker PD-1 did not increase in the three-dimensional microenvironment compared to the two-dimensional environment (Supplementary Fig. 9). Collectively, the peptide hydrogel epitope vaccine not only does not hinder the proliferation of CAR-T cells but also maintains the stability of their functional phenotype, making it a promising vaccine carrier for local T-lymphocyte delivery.

3.3. SPEV-CAR-T promotes DC maturation, T-lymphocyte proliferation and killing

The peptide hydrogel altered antigen delivery and presentation of the E75 epitope vaccine, further affecting the encapsulation of CAR-T cells in situ. We investigated the immunogenicity of SPEV-CAR-T on DC maturation. After 48 h of incubation, DC treated with SPEV-CAR-T showed promising activation, with the percentage of CD86 and MHC I increasing by 2.6-fold and 2.2-fold, respectively (Fig. 4A–C). Additionally, while the peptide hydrogel epitope vaccine activated DC to secrete a small increase in TNF-α and IL-1β, DC activated by SPEV-CAR-T secreted TNF-α and IL-1β by 8.2-fold and 10.4-fold, respectively, aligning with the expression of DC maturation markers (Fig. 4D left column, Fig. 4E and F). These results indicate that SPEV-CAR-T enhances antigen presentation and has a stronger capacity to activate DC.

The strong immunogenicity of the vaccine system contributes to activating cellular and humoral immune responses. To study the ability of SPEV-CAR-T to activate $CD8^+$ T cells through cross-presentation, DCs were treated with either the hydrogel-formulated epitope vaccine or the SPEV-CAR-T vaccine system for 48 h. Then, activated DCs were co-cultured with $CD8^+$ T cells for 72 h to evaluate cell proliferation levels (Fig. 4D middle column). The results showed that DCs pretreated with SPEV-CAR-T promoted $CD8^+$ T cell proliferation by 2.2-fold, higher than the FEFK-E75 epitope vaccine group (1.7-fold, Fig. 4G and H). Moreover, DCs activated by SPEV-CAR-T pretreated $CD8^+$ T cells enhanced the tumor-killing effect and produced significantly higher amounts of IFN-γ and TNF-α than other groups, approximately 2.5–3.2 times higher than the FEFK-E75 epitope vaccine group and 1.3–1.7 times higher than the CAR-T group (Fig. 4I, Supplementary Fig. 10), indicating a stronger ability to promote $CD8^+$ T cell proliferation and activation.

To evaluate the tumor-killing ability of the SPEV-CAR-T system, differently pretreated $CD8^+$ T cells were collected and placed in the aforementioned four microenvironments at different effector-to-target

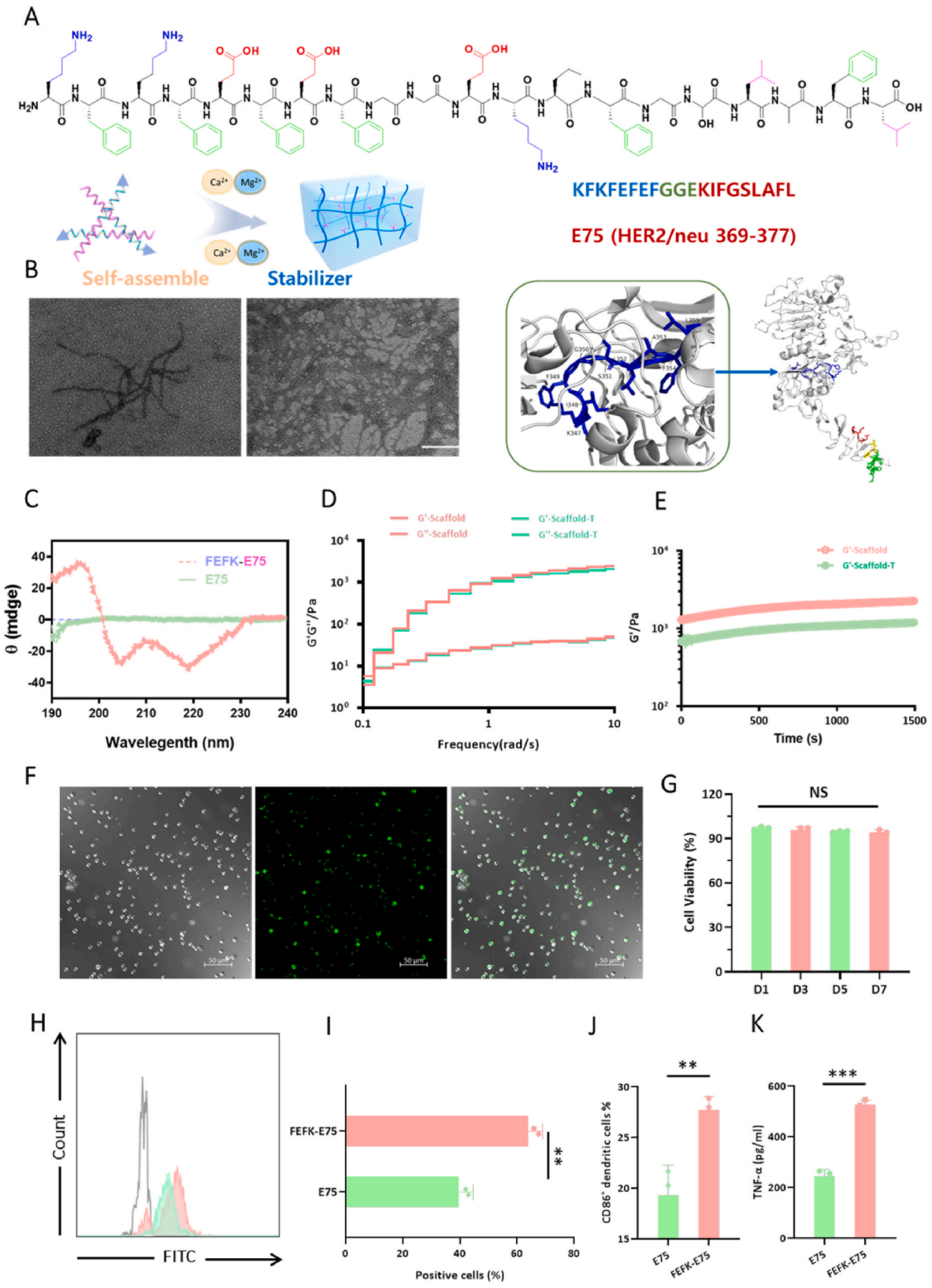

Fig. 2. Preparation and characterization of supramolecular peptide hydrogel epitope vaccine. A, The amino acid sequence of the peptide epitope vaccine FEFK-E75 self-assembles into a hydrogel. B, TEM image of the peptide nanofiber. Scale bars = 200 nm. C, Circular dichroism of FEFK-E75 and E75. D-E, The angular frequency and time of FEFK-E75 with blank or CAR-T cells encapsulated hydrogel (Cell concentration, 1×10^6/mL). F, Micrographs of CAR-T cells cultured in the epitope peptide. Cell viability determined by live-dead assay. G, Viability of CAR-T cells cultured with the epitope peptide each day. H-I, Flow cytometry and percentage of epitope uptake characterized by positive cells after 6 h of treatment. Results normalized to the blank control and E75 group, respectively. J, Fraction of $CD86^+$ DCs after 24 h of culture analyzed by flow cytometry. K, ELISA analysis of TNF-α expression. Results shown as mean ± S.D. from at least three independent experiments. Statistical significance determined by one-way ANOVA with multiple comparisons. $^*P < 0.05$, $^{**}P < 0.01$, $^{***}P < 0.001$. *NS*, not significant.

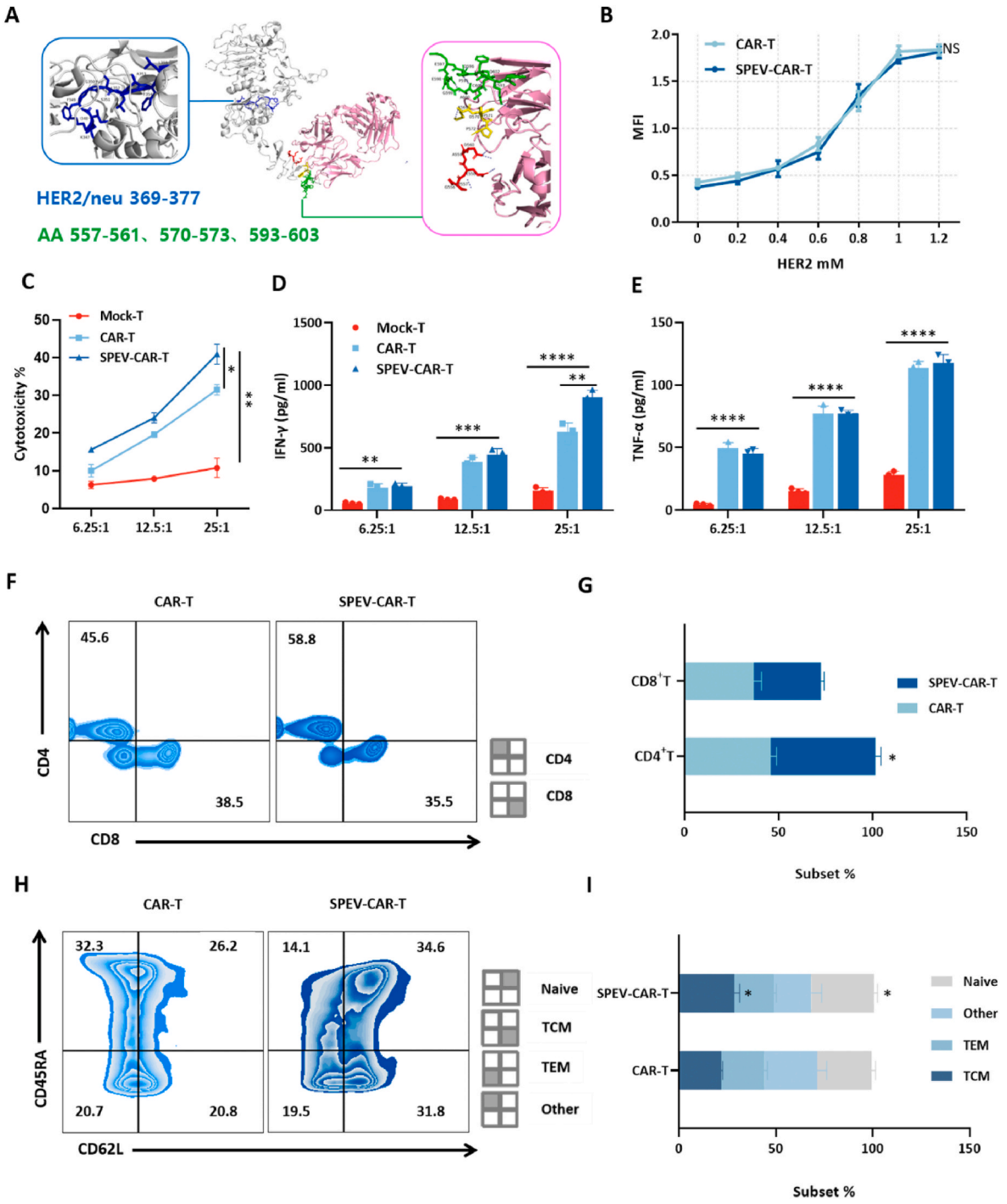

Fig. 3. SPEV-CAR-T promotes CAR-T proliferation and subpopulation transformation. A, Amino acid sequence of E75 peptide and binding sequences of anti-HER2 scFv of CAR-T cells on HER2 protein. B, Affinity of CAR-T to HER2 in peptide hydrogel epitope vaccine or normal medium culture environment. C, Killing effects of SPEV-CAR-T or CAR-T against SKBR3 at different effector-target ratios. D-E, ELISA analyses of IFN-γ and TNF-α expression. F-G, Representative flow cytometry and quantification of $CD4^+$ and $CD8^+$ CAR-T cells. H-I, Representative flow cytometry and quantification of naïve ($CD45RA^+$, $CD62L^+$), central memory T-cells ($CD45RA^-$, $CD62L^+$), and effector memory T-cells ($CD45RA^-$, $CD62L^-$). Results shown as mean ± S.D. from at least three independent experiments. Statistical significance determined by one-way ANOVA with multiple comparisons. $^*P < 0.05$, $^{**}P < 0.01$, $^{***}P < 0.001$, $^{****}P < 0.0001$. *NS*, not significant.

ratios. These cells were then co-cultured with HER2-positive or HER2-negative target cells, and their cytotoxic activity was assessed after 4 h. The supernatant was collected to detect the secretion of cytokines IFN-γ and TNF-α (Fig. 4D right column). DC-activated $CD8^+$ T cells pretreated with the FEFK-E75 epitope vaccine selectively lysed SKBR3 cells (HER2-positive tumor cells), but this effect was weaker than that of the single CAR-T group. Notably, the SPEV-CAR-T pretreated group showed the most significant lysis effect, with a killing effect increased by 29.6 % and 10.0 %, respectively, compared with the FEFK-E75 and CAR-T groups (Fig. 4J). Cytokine secretion was positively correlated with the effector-target ratio (Fig. 4K). Additionally, for MDA-MB-231 (HER2-negative tumor cells), antigen-specific lymphocyte activation and cytokine production were not induced (Fig. 4L and M). These findings confirm that the FEFK-E75 epitope vaccine does not alter the antigen-specific recognition of CAR-T cells but enhances the killing function of endogenous $CD8^+$ T cells, further boosting the cytotoxicity of SPEV-

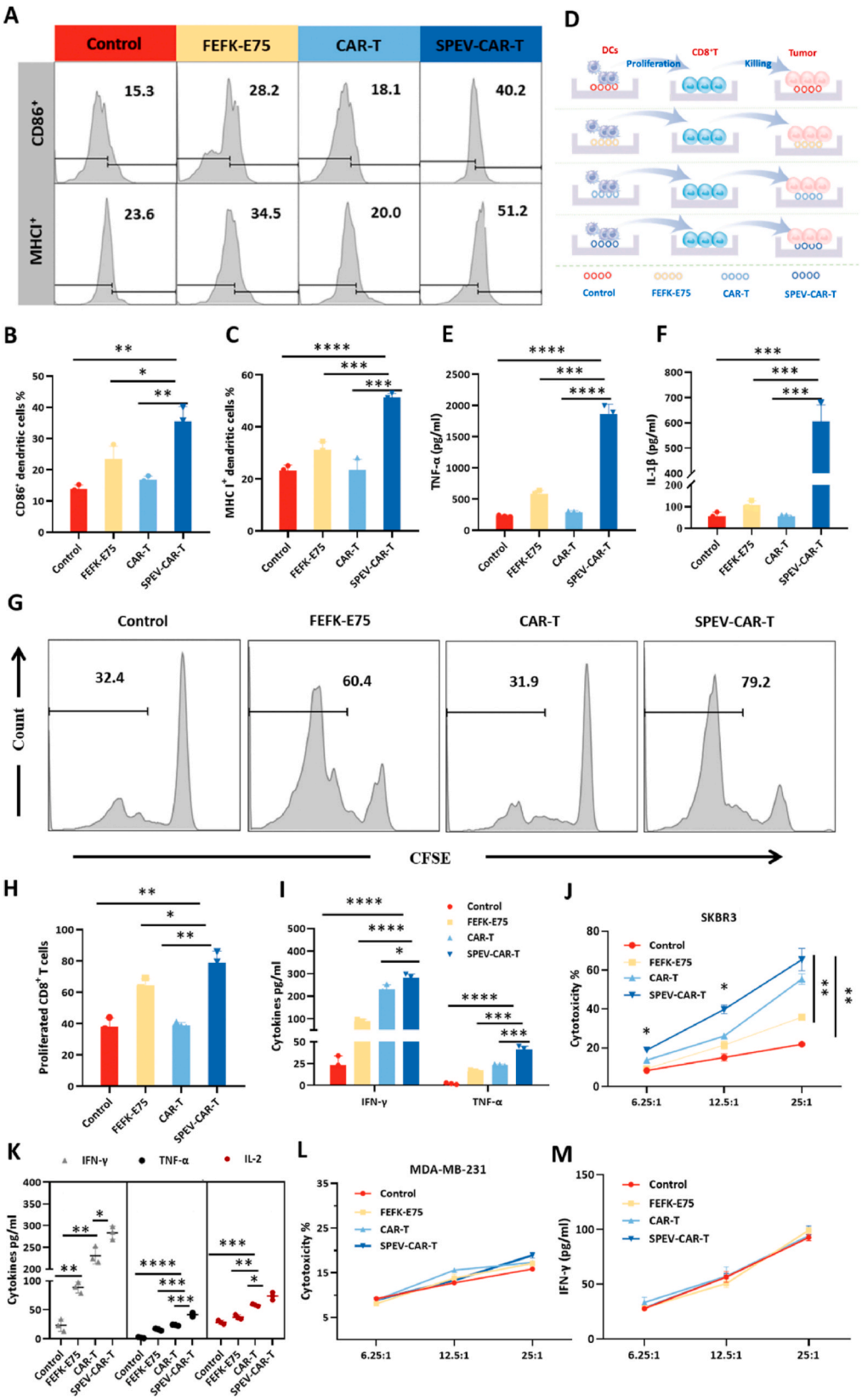

Fig. 4. SPEV-CAR-T promotes DCs maturation, T-lymphocyte proliferation, and killing. A-C, Expression of CD86 and MHC I DCs mature marker in SPEV-CAR-T, FEFK-E75, CAR-T, and normal medium culture environment. D, Schematic illustration of $CD8^{+}$T proliferation and killing stimulated by matured DCs in different culture environments. E-F, Expression levels of TNF-α and IL-1β detected by ELISA. G-H, Representative flow cytometry and quantification of $CFSE^{+}$ $CD8^{+}$T cells. I, Expression levels of IFN-γ and TNF-α detected by ELISA. J, Killing effect of $CD8^{+}$T cells on SKBR3 under different microenvironment. K, Expression levels of IFN-γ, TNF-α, and IL-2 detected by ELISA. L, Killing effect of CAR-T cells on MDA-MB-231 under different effector-target ratios. M, Expression levels of IFN-γ detected by ELISA. Results shown as mean ± S.D. from at least three independent experiments. Statistical significance determined by one-way ANOVA with multiple comparisons. $^{*}P < 0.05$, $^{**}P < 0.01$, $^{***}P < 0.001$, $^{****}P < 0.0001$. *NS*, not significant.

CAR-T.

3.4. The anti-tumor effect of SPEV-CAR-T in therapeutic model of breast cancer

Given the enhanced DC maturation and $CD8^+$ CTL activation by SPEV-CAR-T, we evaluated its anti-tumor effect in a therapeutic mouse model of breast cancer. The experimental protocol is shown in Fig. 5A. At each time point, the mean tumor volume of mice injected with SPEV-CAR-T was smaller than that of the other groups, with a significantly better anti-tumor effect than CAR-T treatment and the FEFK-E75 group (Fig. 5B). This confirmed that subcutaneous injection of SPEV-CAR-T is a potential therapeutic preparation for breast solid tumors.

We first evaluated the tumor infiltration of $CD4^+$ and $CD8^+$ T cells in a tumor-challenging mouse model. Although $CD4^+$ T cells in tumor tissue decreased slightly in the single CAR-T group, the $CD8^+/CD4^+$ T cell ratio was two times higher in the CAR-T group than in others, which is a common prognostic indicator of immunotherapy and clinical success. SPEV-CAR-T maintained high levels of tumor-infiltrating $CD4^+$ and $CD8^+$ T cells (Fig. 5C–E). In addition to directly killing tumor cells, these T lymphocytes secreted various cytokines to activate the immune response, including IFN-γ, TNF-α, and IL-2. IFN-γ is a major cytokine that directly kills tumor cells and is used as an index to evaluate the anti-tumor effect through the number of IFN-γ-secreting T cells. After the second inoculation of SPEV-CAR-T, the frequency of IFN-γ^+ $CD4^+$ T cells (6.0 % higher than that of the FEFK-E75 group) and IFN-γ^+ $CD8^+$ T cells (4.9 % higher than that of the FEFK-E75 group) in tumor-infiltrating lymphocytes significantly increased, as measured by flow cytometry (Fig. 5F–I). These results suggested that SPEV-CAR-T considerably increased the protective cellular immune response.

3.5. SPEV-CAR-T induces antibody dependent humoral immune response

The immunogenicity of epitope peptide vaccines is weak, and they only produce high-valence antibodies when combined with appropriate adjuvants, leading to a strong immune response and lasting memory. We quantified the production of antigen-specific antibodies to investigate the adjuvant effect of SPEV-CAR-T on the humoral immune response in mice. The mice were subcutaneously injected with different preparations on days 7 and 21. The primary and secondary titers of anti-E75 antibodies in serum were detected by ELISA on days 17 and 28. The results showed that on the 17th day of subcutaneous administration, the promotion of antibodies in FEFK-E75 was not obvious, while SPEV-CAR-T promoted the production of anti-HER2 IgG by 9.2-fold, IgG1 by 7.2-fold, and IgG2c by 20.0-fold, significantly better than the FEFK-E75 group (Fig. 6A). This indicates that FEFK-E75-based vaccines were insufficient to trigger a rapid, strong antigen-specific antibody response after a single dose. SPEV-CAR-T showed a high level of antibody protection in the early stage, which may explain the better anti-tumor effect.

For antibody titers after the second immunization, SPEV-CAR-T showed a 19.5-fold increase in anti-HER2 IgG compared to the control. Additionally, SPEV-CAR-T enhanced anti-HER2 IgG1 by 13.0-fold compared to the control, close to free FEFK-E75. Surprisingly, SPEV-CAR-T significantly increased anti-HER2 IgG2c by 27.3-fold (Fig. 6B). This indicates that SPEV-CAR-T elicits a strong humoral immune response after a second dose. The spleen index of mice can partly explain the vaccine's stimulating effect on the immune system. Therefore, the spleen was taken on the fourth day after the last immunization, and the spleen index was calculated. The results, shown in Fig. 6C, indicate that KKEF-E75 and SPEV-CAR-T significantly stimulated spleen proliferation. In the anti-tumor immune response, cytokine production is highly correlated with the specific T-cell response, including IL-4, IL-5 (Th2-type cytokines), and IFN-γ (Th1-type cytokines). The expression of cytokines in the serum of mice 7 days after the last inoculation of SPEV-CAR-T was detected. Compared with the FEFK-E75 group, the level of IFN-γ in mice treated with SPEV-CAR-T increased significantly by 5–6 fold, while the increase in IL-4 and IL-5 was not significant, consistent with the effects of IgG2c and IgG1 antibody isotypes (Fig. 6D). In summary, the peptide hydrogel epitope vaccine encapsulating CAR-T cells effectively enhanced the immune response to the E75 protein in vivo.

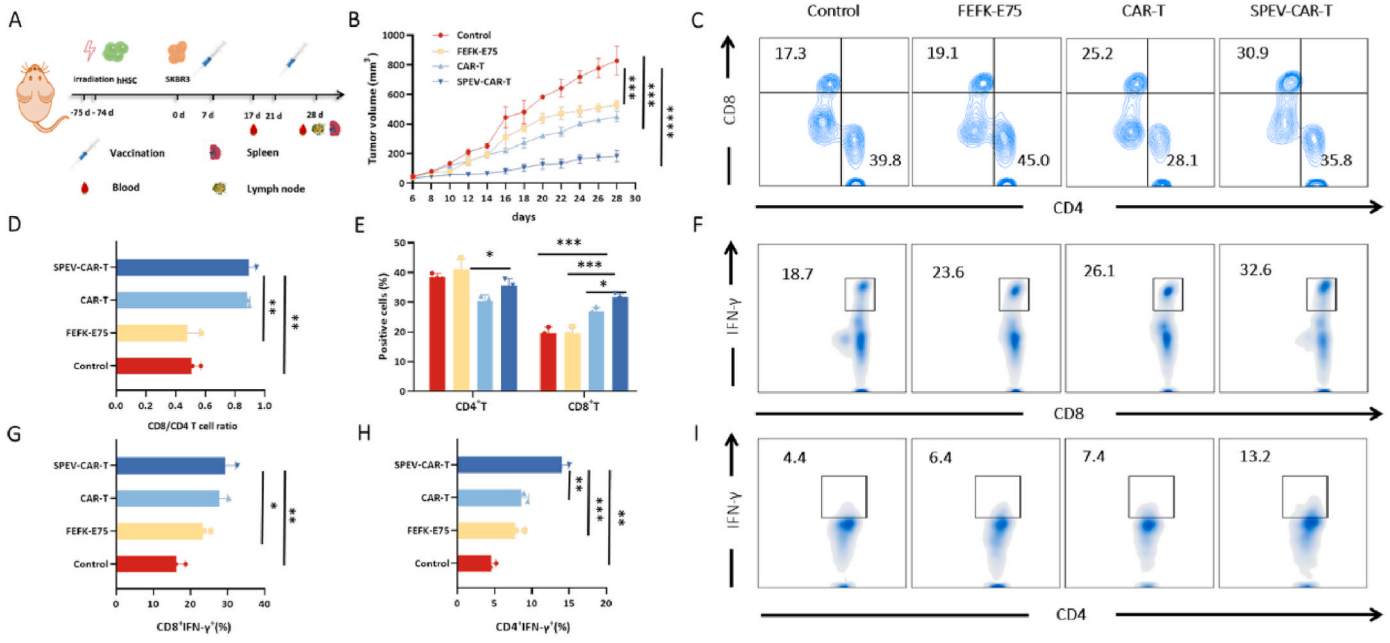

Fig. 5. Anti-tumor effect of SPEV-CAR-T in therapeutic model of breast cancer. A, Scheme of experimental protocol. B, Monitoring of SKBR3 tumor volume and curves drawn (n = 4 animals/group). C-E, Representative flow cytometry and quantification of tumor-infiltrating $CD4^+$ T and $CD8^+$ T cells. F-I, Representative flow cytometry and quantification of tumor-infiltrating IFN-γ^+CD4^+ T and IFN-γ^+CD8^+ T cells. Results shown as mean ± S.D. from at least three independent experiments. Statistical significance determined by one-way ANOVA with multiple comparisons. $^*P < 0.05$, $^{**}P < 0.01$, $^{***}P < 0.001$, $^{****}P < 0.0001$.

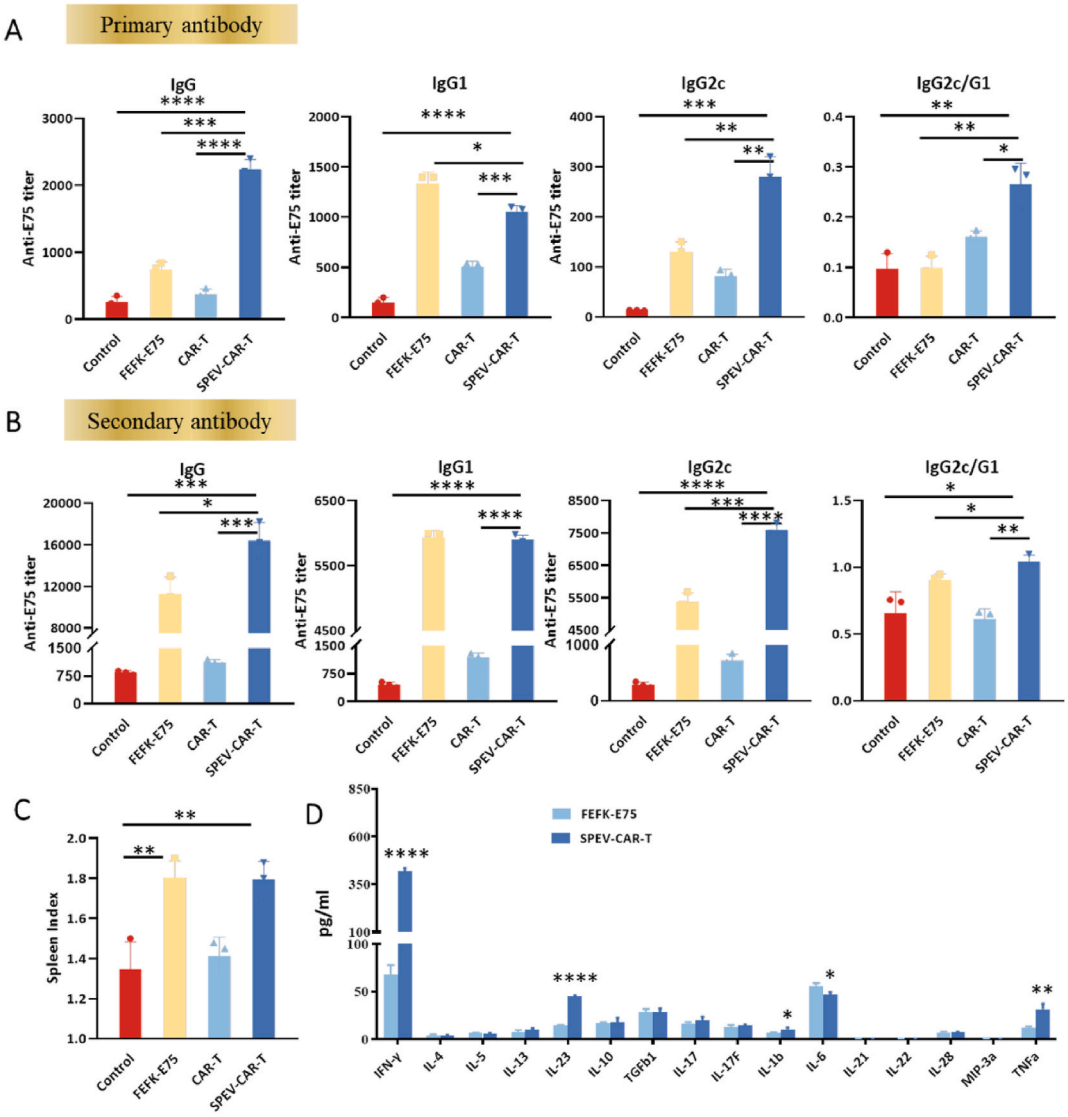

Fig. 6. SPEV-CAR-T induces antibody-dependent humoral immune response. A, Primary IgG, IgG1, and IgG2c antibody titers and IgG2c/IgG1 ratio 10 days after the first immunization. B, IgG, IgG1, and IgG2c antibody titers and IgG2c/IgG1 ratio 7 days after the second immunization. C, Spleen index in mice inoculated with different preparations (n = 4 animals/group). D, Cytokine levels detected by Proteome Profiler Array. Results shown as mean ± S.D. from at least three independent experiments. Statistical significance determined by one-way ANOVA with multiple comparisons. *P < 0.05, **P < 0.01, ***P < 0.001, ****P < 0.0001.

3.6. SPEV-CAR-T induces persistent and systematic cellular immune response

The peptide hydrogel epitope vaccine is susceptible to protease degradation in vivo, and CAR-T cells released from SPEV-CAR-T kill tumors directly. Compared to the high-dose injection of CAR-T cells into the blood, SPEV-CAR-T sustains and slowly reaches the local tumor, leading to higher efficiency and lower cytotoxicity. The hydrogel provides a reservoir for CAR-T cells, maintaining long-lasting anti-tumor effects. In this study, CAR-T cells were labeled with luciferase, encapsulated into the hydrogel epitope vaccine, and injected subcutaneously into mice. Fluorescent images were recorded at indicated time points, with individual CAR-T cells used as the control group. By day 7, almost all individual CAR-T cells were released, while SPEV-CAR-T maintained approximately 50 % in situ (Fig. 7A and B). The released CAR-T cells naturally homed to the tumor and lymph nodes, counted at the indicated time points. The CAR-T cells in the control group declined on day 4, while they expanded in the hydrogel epitope vaccine group until day 10 (Supplementary Fig. 11). The peptide hydrogel scaffold played a crucial role in CAR-T cell proliferation, and the slow release further improved the durability of SPEV-CAR-T.

Lymph nodes are the predominant location of the immune response, where efficient antigen delivery recruits antigen-presenting cells and activates antigen-specific immune cells throughout the body. We detected the recruitment and activation of immune cells by flow cytometry. Compared with other treatment groups, both SPEV-CAR-T and FEFK-E75 significantly promoted the accumulation of $CD11c^+$ cells in lymph nodes (Supplementary Fig. 12). However, SPEV-CAR-T induced DC maturation more effectively than FEFK-E75, as evidenced by the maturation markers CD80 and CD86 (Fig. 7C–E). Taken together, these results suggest that SPEV-CAR-T enhances DC recruitment and maturation, initiating the activation of endogenous lymphocytes. Next, we investigated the ability of SPEV-CAR-T to activate lymphocytes in the draining lymph nodes and spleen. $CD8^+$ T cells promote antigen-specific cytotoxicity. The results showed that SPEV-CAR-T increased $CD69^+CD3^+CD8^+$ T cells by 1.4–1.7 fold in the spleen and lymph nodes compared with CAR-T groups. Additionally, SPEV-CAR-T activated $CD4^+$ T cells by 5.8 fold in the lymph nodes compared to the FEFK-E75 group. $CD4^+$ T cells not only enhance the tumor-killing effect of $CD8^+$ T cells by regulating and coordinating the immune response but also

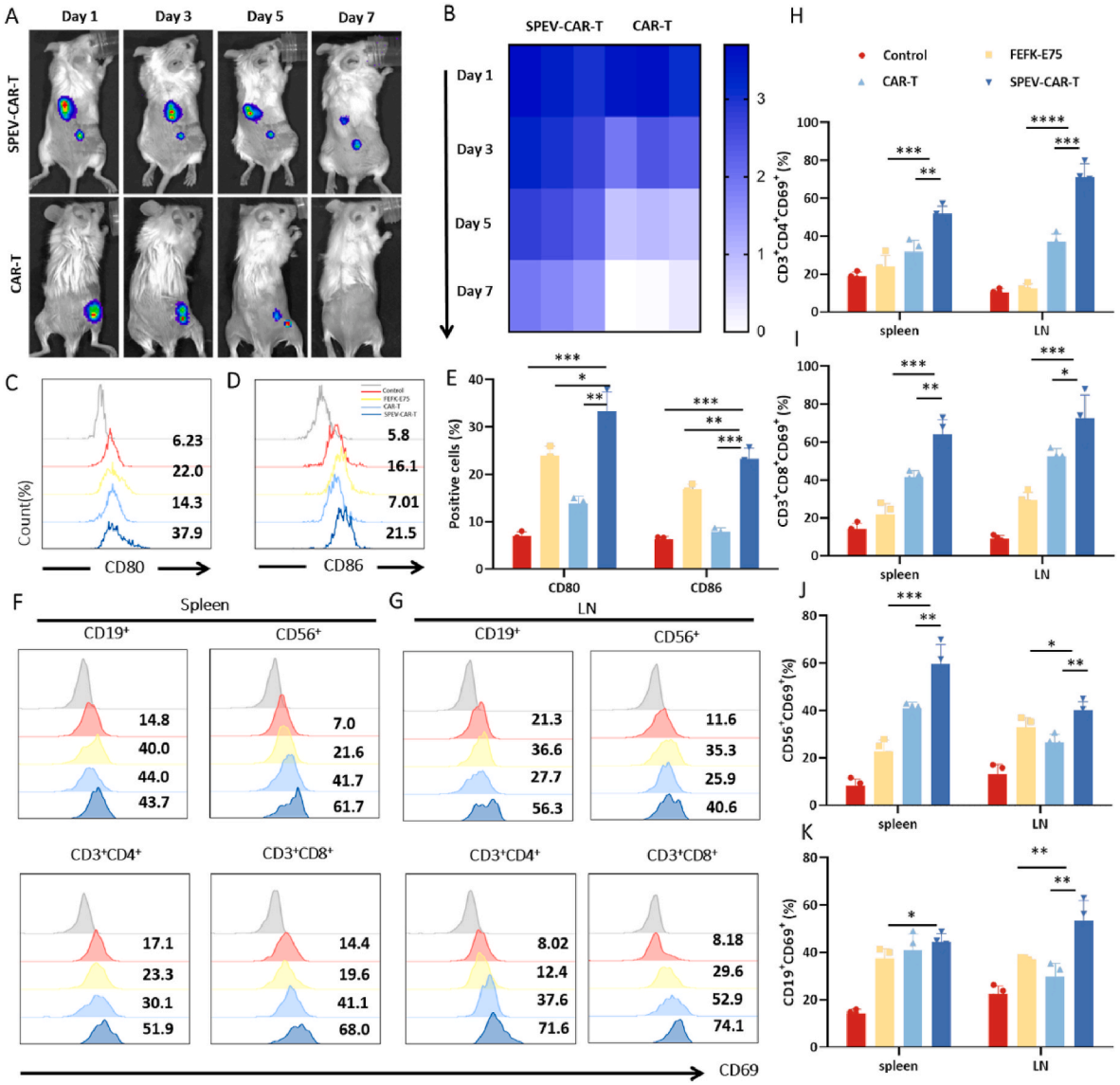

Fig. 7. SPEV-CAR-T induces persistent and systematic cellular immune response. A-B, Imaging and quantification of Luc-labeled CAR-T with or without hydrogel scaffolds daily (n = 3 animals/group). C-E, Flow cytometric histogram and quantification of $CD80^+$ and $CD86^+$ DCs in lymph nodes. F-G, Flow cytometric histogram of B, NK, $CD4^+$, and $CD8^+$ T cells activated marker in spleen and lymph nodes. H-K, Proportion of B, NK, $CD4^+$, and $CD8^+$ T cells activated marker in spleen and lymph nodes. Results shown as mean ± S.D. from at least three independent experiments. Statistical significance determined by one-way ANOVA with multiple comparisons. $^*P < 0.05$, $^{**}P < 0.01$, $^{***}P < 0.001$.

promote the production of memory cells to form a durable immune response to tumors. Meanwhile, SPEV-CAR-T showed higher activated B cells than other groups, consistent with elevated serum anti-HER2 IgG titers. Furthermore, the number of $CD69^+$ NK cells in the SPEV-CAR-T group increased by 1.5–1.6 fold compared with the CAR-T group (Fig. 7F–K). Taken together, these results indicate that the peptide hydrogel epitope vaccine, as a delivery vector, promotes CAR-T cell proliferation and targeting. Additionally, the peptide hydrogel as a vaccine adjuvant effectively prolongs vaccine exposure time and recruits antigen-presenting cells, enhancing the immune response in lymph nodes and leading to systemic anti-tumor effects.

3.7. *SPEV-CAR-T induces lasting and protective memory T-cell responses*

In general, memory T cells increase after effective vaccination, triggering a quicker and higher magnitude immune response when a specific antigen reappears. In a preventive breast cancer model, mice were challenged with a tumor 7 days after the second vaccination. The phenotype and activation of T cells in the spleen were analyzed by flow cytometry 4 days after tumor challenge. The memory T-cell compartment was subdivided into central memory T cells (TCM, $CD45RA^-$ $CD62L^+$), effector memory T cells (TEM, $CD45RA^-$ $CD62L^-$), and naive T cells (Naive, $CD45RA^+$ $CD62L^+$). The results showed that SPEV-CAR-T induced higher proportions of TCM compared to other groups (Fig. 8A and B). Additionally, markers of activation, CD69 and CD25, were higher in the experimental group (Fig. 8C).

Long-term antigen stimulation eventually induces T-cell exhaustion, characterized by reduced cell numbers, decreased cytokine production, and up-regulated inhibitory receptors, including PD-1, Lag3, and CTLA-4. In our study, tumor-infiltrating lymphocytes were collected to further evaluate the expression of PD-1, a marker of T-cell exhaustion. The results showed that the SPEV-CAR-T group expressed lower levels of PD-1 (Fig. 8D and E). Furthermore, the expression levels of IFN-γ, TNF-α, and IL-2 isolated from blood were evaluated. The SPEV-CAR-T group was slightly higher than the CAR-T group and significantly higher than the FEFK-E75 group (Fig. 8F–H). Meanwhile, the SPEV-CAR-T group

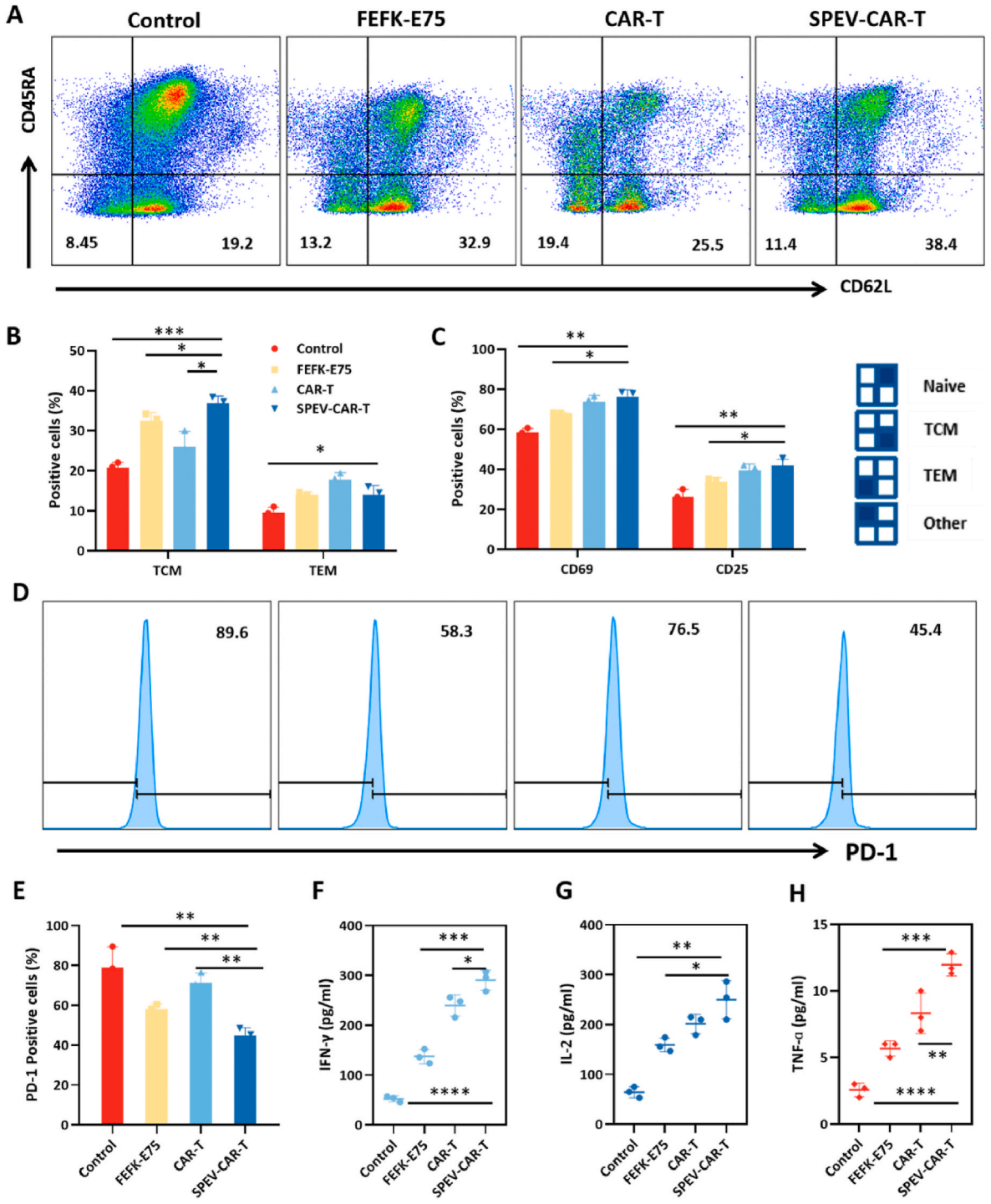

Fig. 8. SPEV-CAR-T induces lasting and protective memory T-cell. A, Representative flow cytometry and quantification of naïve ($CD45RA^{+}$, $CD62L^{+}$), central memory T-cells ($CD45RA^{-}$, $CD62L^{+}$), and effector memory T-cells ($CD45RA^{-}$, $CD62L^{-}$) in spleen. B-C, Quantitative analysis of CD25 or CD69 positive cells. D-E, Representative flow cytometry and quantitative analysis of PD-1 expression on tumor-infiltrating T cells. F-H, Expression of representative cytokines IFN-γ, IL-2, and TNF-α in blood. Results shown as mean ± S.D. from at least three independent experiments. Statistical significance determined by one-way ANOVA with multiple comparisons. $^{*}P < 0.05$, $^{**}P < 0.01$, $^{***}P < 0.001$, $^{****}P < 0.0001$.

exhibited the most delayed tumor growth rate (Supplementary Fig. 13). These results indicate that the peptide hydrogel environment delays T cells' transition into the dysfunction phase. SPEV-CAR-T forms a higher proportion of central memory T cells and cytokines for tumor killing. Additionally, the hydrogel epitope vaccine provides a suitable shelter for tumor-infiltrating lymphocytes to survive at the tumor site, maintaining a high level of lymphocyte response.

4. Discussion

In recent years, CAR-T treatments have shown remarkable performance in various tumors, especially hematologic ones, and new CAR-T targets continue to emerge, bringing new hope to patients [2,10]. Currently, there are five CAR-T products approved by the FDA for treating hematologic tumors. Additionally, a new product targeting B cell maturation antigen (BCMA) has been approved for treating multiple

myeloma [6,27]. Despite these clinical successes, the efficiency of CAR-T in solid tumors remains unsatisfactory due to barriers such as tumor heterogeneity, off-target effects, limited CAR-T cell expansion and persistence, and challenges in tumor infiltration and microenvironment [1,28,29]. Considering the high complexity of solid tumors, it is challenging to balance these factors with CAR-T alone. In our previous study, we developed customized immune cell matrix scaffolds based on self-assembling peptides to preserve and augment the cell phenotype according to the characteristics of CAR-T cells. These mimic matrix scaffolds showed optimal stiffness and adhesive ligand density, thereby accelerating CAR-T-cell proliferation [4]. This study focuses on improving the targeted efficiency and persistence of CAR-T in solid tumor treatment based on previous findings.

Combined targeted treatment is an effective strategy for solid tumors. However, CAR-T combined with immune checkpoint inhibitors or antibodies has certain limitations according to several preclinical experiments [30–32]. While tumors were killed, the consequences of systemic cytokine storm syndrome were severe [32]. Malignant tumors are characterized by invasion and recurrence, necessitating better-targeted and less toxic treatments. CAR-T combined with tumor vaccines shows promising potential in clinical applications by recruiting and activating the patient's own immune cells to induce a stronger anti-tumor effect [17]. In this study, active and passive immune responses were integrated and complemented in all-in-one hydrogel epitopes vaccine and CAR-T system. The sequential succession of endogenous and exogenous immune responses promoted persistent and specific tumor attack and showed superior therapeutic effect in solid tumors.

Peptide vaccines have the advantages of strong specificity and high safety, precisely targeting HER2, a major focus in breast cancer. The E75 epitope, located at positions 369–377 of the HER2 protein, induces an effective anti-HER2 immune response when combined with the adjuvant granulocyte-macrophage colony-stimulating factor (GM-CSF) [33,34]. Additionally, various biomaterials have been designed and used as new adjuvants for E75 to promote immunogenicity [35,36]. The self-assembled short peptide hydrogel, as a new material, has broad application prospects in tissue engineering and immunotherapy due to its high biocompatibility and easy design and synthesis [23,37]. Previous studies have found that short peptide self-assembly hydrogels are effective immune adjuvants, significantly inducing immune responses when linked with epitope peptides [24]. In Tirrell's study, self-assembled peptide amphiphiles delivering cytotoxic T-cell epitopes induced a strong immune response in mice [38]. Our previously developed synthetic, supramolecular, and self-adjuvanting $CD8^+$ T cell epitope vaccine induced DC maturation and therapeutic antitumor immunity, outperforming the conventional adjuvant MF59 group [24]. In this research, self-assembled peptides linked with the E75 epitope preserved the full function of CAR-T cells and increased the immunogenicity of E75, significantly improving antibody levels as adjuvants. Sustained exposure of the hydrogel epitope to secondary lymphoid tissue led to the recruitment of immune cells and established systemic specific protection against tumor antigens. The local microenvironment promoted APC uptake, immune cell activation, adaptive immune response initiation, and immune memory formation. During anti-tumor treatment, the level of cellular immune response, represented by IgG2c, was greatly improved, along with the formation of central memory cells, leading to a faster, stronger, and more durable immune response. These effects are likely attributable to the self-assembling peptide KFKFEFEF, which modifies the characteristics of E75, including its surface charge, nanomaterial physical properties, and cellular uptake and release pathways. It is more probable that these outcomes result from a synergistic combination of multiple mechanisms.

Single-target CAR-T cells are unable to cope with tumor escape due to antigen loss or down-regulation [39]. The E75 epitope and CAR-T target sites are from different extracellular domains of the HER2 protein. This design targets different sites of the same antigen, alleviating antigen modulation. Vaccine-driven antigen diffusion allows the body's immune system to collaborate with CAR-T cells, rather than being limited to attacking tumor cells expressing CAR-T-targeted antigens. In Irvine's study, vaccines using the same target antigen after CAR-T treatment greatly improved the effectiveness of treatment in glioma, making this approach more likely to eradicate solid tumors [17]. In this study, SPEV-CAR-T enhanced the recruitment of DCs to the lymph nodes, triggering the activation of endogenous T, B, and NK cells. Both endogenous lymphocytes and CAR-T cells significantly contributed to improving tumor-killing efficiency.

Another major obstacle for CAR-T treatment in solid tumors is the inability to accumulate and expand at the tumor site via intravenous injection. The abundance of blood vessels and tumor-associated fibroblasts forms a natural physical barrier that prevents cells from entering solid tumors [6,40,41]. Additionally, the lack of chemokine receptor expression in CAR-T cells reduces their homing ability to the tumor site. Local regional delivery of CAR-T cells may be a more effective treatment strategy [42–45]. Optimizing the delivery vector is an approach worth exploring. Biomaterial scaffolds have advantages such as easy preparation, good biocompatibility, and high safety, showing good prospects in drug or cell delivery. Our previous study validated that short peptide hydrogels maintained the activity and complete biological function of CAR-T cells when injected into the body [4]. Local cell release reduced the journey of intravenous infusion, shortened the time of tumor infiltration, and maximized the viability of CAR-T cells. Additionally, cells were sustainedly released from the hydrogel and lodged at the tumor site, providing a steady supply of reinforcements for attacking tumors and avoiding cytokine storms caused by a single high dose.

Immunosuppression in the tumor microenvironment affects the antitumor efficacy of CAR-T cells, primarily through inhibitory cytokines such as IL-10 and TGF-β, and other cytokines secreted by various immunosuppressive cells (Treg, MDSC, or M2) [26,46,47]. Armored CAR-T cells utilize cytokines like IL-12 and IL-18 to enhance anti-tumor efficacy. Studies have shown that IL-12 can break immune suppression in ovarian cancer, improving the survival and proliferation of CAR-T cells [48]. IL-18-secreting CAR-T cells can improve the tumor microenvironment by recruiting more endogenous immune cells and increasing the expression of immune activators. In our research, epitope vaccines were introduced to stimulate endogenous lymphocytes. The nano-vaccine delivers the antigen to APCs in the spleen and lymph nodes. Activated DCs secrete IL-12, activating and expanding antigen-specific T lymphocytes and enhancing B/NK cells. The crosstalk between cytokines IL-12 and IFN-γ, secreted by activated lymphocytes and APCs, is an important positive feedback loop in generating effective responses in numerous successful immunotherapies. Additionally, the self-assembled peptide hydrogel epitope vaccine is a scalable functional system, capable of encapsulating cytokines as needed to support a moderate living environment for CAR-T cells. In this study, Ca^{2+}/Mg^{2+} ions were encapsulated in the hydrogel as stabilizers, which also maintained the proliferation and differentiation of CAR-T cells and induced the formation of memory cells in vivo. Previous studies indicated that low serum magnesium levels are associated with worse outcomes in cancer immunotherapy by regulating effector-memory $CD8^+$ T cells [49]. The SPEV-CAR-T system significantly enhance the expression of DCs surface maturation markers while promoting the secretion of inflammatory cytokines by DCs. This effect relies on both direct and indirect factors. The direct factors include the ability of the E75 epitope in the SPEV-CAR-T system to continuously stimulate DCs, promoting their maturation. This process is further strengthened by direct cell-to-cell contact, which enhances the activation and immune functions of DCs. Simultaneously, SPEV-CAR-T through the expression of immune co-stimulatory molecules, interact with receptors on the surface of DCs, providing a second signal to promote DCs maturation. On the other hand, in terms of indirect effects, SPEV-CAR-T co-cultured with DCs release immune-regulatory factors (IFN-γ and TNF-α), which directly or indirectly activate DCs and facilitate their transformation into a mature phenotype. These factors enhance the antigen-presenting

function of DCs, boost their immune responses, and improve their ability to activate T cells.

5. Conclusion

A novel target combination immunotherapy strategy based on a supramolecular peptide hydrogel epitopes vaccine functionalized with CAR-T cells was studied. First, the self-assembled peptide coupling with the E75 epitope formed a nanofiber scaffold through non-covalent interactions of amphiphilic amino acids. The complementary peptide-conjugated vaccine epitopes and CAR-T target sites are from different extracellular domains of the HER2 protein, and this combination therapy improves tumor antigen spreading and targeting efficiency. The epitope hydrogel promoted CAR-T cell proliferation, killing, and lymphocyte subpopulation transformation. Furthermore, the supramolecular peptide epitope vaccine encapsulating CAR-T cells drove endogenous humoral and cellular immune responses following a sustained release of the hydrogel and CAR-T cells, showing better antitumor effects in an in vivo mouse model. Most importantly, SPEV-CAR-T induced central memory cells in systemic immune tissues, addressing the poor persistence of single CAR-T treatment. Active and passive immune responses were integrated and complemented in the all-in-one hydrogel epitopes vaccine and CAR-T system. The sequential activation of endogenous and exogenous immune responses promoted persistent and specific tumor attack, and SPEV-CAR-T showed superior therapeutic effects in solid tumors.

CRediT authorship contribution statement

Pengxiang Yang: Writing – review & editing, Supervision, Funding acquisition, Conceptualization. **Xiaomin Yao:** Formal analysis, Data curation. **Xue Tian:** Formal analysis, Data curation. **Yuehan Wang:** Formal analysis, Data curation. **Leilei Gong:** Writing – review & editing, Funding acquisition. **Yumin Yang:** Writing – review & editing, Funding acquisition. **Jing Jie:** Writing – review & editing, Funding acquisition, Formal analysis.

Ethics approval and consent to participate

All animal experiments were approved by the Ethics Committee of Nantong University (Nantong, China; approval No. S20220220-009). All authors were compliance with all relevant ethical regulations.

Funding

We want to acknowledge the financial support received from the National Key R&D Program of China (No.2022YFC2409800, 2022YFC2409802), National Natural Science Foundation of China (No. 32271389, 32230057, 31900987), Jiangsu Natural Science Foundation (No. BK20230608), Nantong Science and Technology Plan Project (No. MSZ2022196), Nantong University innovative training program (No.2024007CX).

Declaration of competing interest

No conflicts of interest exist related to the submission of this manuscript.

Appendix A. Supplementary data

Supplementary data to this article can be found online at https://doi.org/10.1016/j.mtbio.2025.101517.

Data availability

Data will be made available on request.

References

[1] I. Zhu, R. Liu, J.M. Garcia, A. Hyrenius-Wittsten, D.I. Piraner, J. Alavi, D.V. Israni, B. Liu, A.S. Khalil, K.T. Roybal, Modular design of synthetic receptors for programmed gene regulation in cell therapies, Cell 185 (8) (2022) 1431–1443.e16.
[2] D.J. Baker, Z. Arany, J.A. Baur, J.A. Epstein, C.H. June, CAR T therapy beyond cancer: the evolution of a living drug, Nature 619 (7971) (2023) 707–715.
[3] R. Li, C. Ma, H. Cai, W. Chen, The CAR T-cell mechanoimmunology at a glance, Adv. Sci. 7 (24) (2020) 2002628.
[4] J. Jie, D. Mao, J. Cao, P. Feng, P. Yang, Customized multifunctional peptide hydrogel scaffolds for CAR-T-cell rapid proliferation and solid tumor immunotherapy, ACS Appl. Mater. Interfac. 14 (33) (2022) 37514–37527.
[5] P. Yang, X. Cao, H. Cai, X. Chen, Y. Zhu, Y. Yang, W. An, J. Jie, Upregulation of microRNA-155 enhanced migration and function of dendritic cells in three-dimensional breast cancer microenvironment, Immunol. Invest. 50 (8) (2020) 1058–1071.
[6] Z.T. Li, Y.X. Wang, Y.Y. Ding, L. Repp, G.S. Kwon, Q.Y. Hu, Cell-based delivery systems: emerging carriers for immunotherapy, Adv. Funct. Mater. (2021) 32.
[7] F. Xie, X. Zhou, M. Fang, H. Li, P. Su, Y. Tu, L. Zhang, F. Zhou, Extracellular vesicles in cancer immune microenvironment and cancer immunotherapy, Adv. Sci. 6 (24) (2019) 1901779.
[8] U. Uslu, T. Da, C.-A. Assenmacher, J. Scholler, R.M. Young, J. Tchou, C.H. June, Chimeric antigen receptor T cells as adjuvant therapy for unresectable adenocarcinoma, Sci. Adv. 9 (2) (2023) eade2526.
[9] E. Seung, Z. Xing, L. Wu, E. Rao, V. Cortez-Retamozo, B. Ospina, L. Chen, C. Beil, Z. Song, B. Zhang, M. Levit, G. Deng, A. Hebert, P. Kirby, A. Li, E.J. Poulton, R. Vicente, A. Garrigou, P. Piepenhagen, G. Ulinski, M. Sanicola-Nadel, D. S. Bangari, H. Qiu, L. Pao, D. Wiederschain, R. Wei, Z.Y. Yang, G.J. Nabel, A trispecific antibody targeting HER2 and T cells inhibits breast cancer growth via CD4 cells, Nature 603 (7900) (2022) 328–334.
[10] Q. Xiao, X. Zhang, L. Tu, J. Cao, C.S. Hinrichs, X. Su, Size-dependent activation of CAR-T cells, Sci. Immunol. 7 (74) (2022) eabl3995.
[11] S. Sun, Z. Ding, L. Gao, B.D. Hammock, X. Huang, Z.P. Xu, X. Wang, Q. Cheng, F. Mo, W. Shi, S. Xie, A. Liu, H. Li, X. Yang, X. Lu, A dendritic/tumor fusion cell vaccine enhances efficacy of nanobody-based CAR-T cells against solid tumor, Theranostics 13 (14) (2023) 5099–5113.
[12] L. Liu, J. Chen, J. Bae, H. Li, Z. Sun, C. Moore, E. Hsu, C. Han, J. Qiao, Y.X. Fu, Rejuvenation of tumour-specific T cells through bispecific antibodies targeting PD-L1 on dendritic cells, Nat. Biomed. Eng. 5 (11) (2021) 1261–1273.
[13] P. Yang, H. Song, Y. Qin, P. Huang, C. Zhang, D. Kong, W. Wang, Engineering dendritic-cell-based vaccines and PD-1 blockade in self-assembled peptide nanofibrous hydrogel to amplify antitumor T-cell immunity, Nano Lett. 18 (7) (2018) 4377–4385.
[14] H. Hao, S. Wu, J. Lin, Z. Zheng, Y. Zhou, Y. Zhang, Q. Guo, F. Tian, M. Zhao, Y. Chen, X. Xu, L. Hou, X. Wang, R. Tang, Immunization against Zika by entrapping live virus in a subcutaneous self-adjuvanting hydrogel, Nat. Biomed. Eng. 7 (7) (2023) 928–942.
[15] A.J. Najibi, M.O. Dellacherie, T.-Y. Shih, E.J. Doherty, D.A. White, T. Bauleth-Ramos, A.G. Stafford, J.C. Weaver, C.D. Yeager, B.T. Seiler, M. Pezone, A.W. Li, B. Sarmento, H.A. Santos, D.J. Mooney, L. Gu, Scaffold vaccines for generating robust and tunable antibody responses, Adv. Funct. Mater. 32 (16) (2022) 2110905.
[16] L. Sun, F. Shen, Z. Xiong, H. Yang, Z. Dong, J. Xiang, Q. Gu, Q. Ji, C. Fan, Z. Liu, DNA engineered lymphocyte-based homologous targeting artificial antigen-presenting cells for personalized cancer immunotherapy, J. Am. Chem. Soc. 144 (17) (2022) 7634–7645.
[17] L. Ma, T. Dichwalkar, J.Y.H. Chang, B. Cossette, D. Garafola, A.Q. Zhang, M. Fichter, C. Wang, S. Liang, M. Silva, S. Kumari, N.K. Mehta, W. Abraham, N. Thai, N. Li, K.D. Wittrup, D.J. Irvine, Enhanced CAR-T cell activity against solid tumors by vaccine boosting through the chimeric receptor, Science (New York, N. Y.) 365 (6449) (2019) 162–168.
[18] K. Reinhard, B. Rengstl, P. Oehm, K. Michel, A. Billmeier, N. Hayduk, O. Klein, K. Kuna, Y. Ouchan, S. Wöll, E. Christ, D. Weber, M. Suchan, T. Bukur, M. Birtel, V. Jahndel, K. Mroz, K. Hobohm, L. Kranz, M. Diken, K. Kühlcke, Ö. Türeci, U. Sahin, An RNA vaccine drives expansion and efficacy of claudin-CAR-T cells against solid tumors, Science 367 (6476) (2020) 446–453.
[19] A. Singh, Genome-wide high-throughput screening of T cell epitopes, Nat. Methods 16 (10) (2019) 953.
[20] A. Ukidve, K. Cu, M. Goetz, P. Angsantikul, A. Curreri, E.E.L. Tanner, J. Lahann, S. Mitragotri, Ionic-liquid-based safe adjuvants, Adv. Mater. 32 (46) (2020) e2002990.
[21] L. Zhang, D. Jing, N. Jiang, T. Rojalin, C.M. Baehr, D. Zhang, W. Xiao, Y. Wu, Z. Cong, J.J. Li, Y. Li, L. Wang, K.S. Lam, Transformable peptide nanoparticles arrest HER2 signalling and cause cancer cell death in vivo, Nat. Nanotechnol. 15 (2) (2020) 145–153.
[22] Q. Su, H. Song, P. Huang, C. Zhang, J. Yang, D. Kong, W. Wang, Supramolecular co-assembly of self-adjuvanting nanofibrious peptide hydrogel enhances cancer vaccination by activating MyD88-dependent NF-κB signaling pathway without inflammation, Bioact. Mater. 6 (11) (2021) 3924–3934.
[23] P. Yang, Y. Peng, X. Dai, J. Jie, D. Kong, X. Gu, Y. Yang, Bionic peptide scaffold in situ polarization and recruitment of M2 macrophages to promote peripheral nerve regeneration, Bioact. Mater. 30 (2023) 85–97.
[24] P. Yang, H. Song, Z. Feng, C. Wang, P. Huang, C. Zhang, D. Kong, W. Wang, Synthetic, supramolecular, and self-adjuvanting CD8+ T-cell epitope vaccine increases the therapeutic antitumor immunity, Adv. Therapeut. 2 (7) (2019) 1900010.

[25] L.S. Shores, S.H. Kelly, K.M. Hainline, J. Suwanpradid, A.S. MacLeod, J.H. Collier, Multifactorial design of a supramolecular peptide anti-IL-17 vaccine toward the treatment of psoriasis, Front. Immunol. 11 (2020) 1855.
[26] P. Yang, X. Cao, H. Cai, P. Feng, X. Chen, Y. Zhu, Y. Yang, W. An, Y. Yang, J. Jie, The exosomes derived from CAR-T cell efficiently target mesothelin and reduce triple-negative breast cancer growth, Cell. Immunol. 360 (2021) 104262.
[27] N. Eckman, A. Nejatfard, R. Cavet, A.K. Grosskopf, E.A. Appel, Biomaterials to enhance adoptive cell therapy, Nature Rev. Bioeng. (2024).
[28] D. Zhang, Q. Li, X. Chen, X. Nie, F. Xue, W. Xu, Y. Luan, An injectable hydrogel to modulate T cells for cancer immunotherapy, Small 18 (32) (2022) e2202663.
[29] X. Li, T. Zhu, R. Wang, J. Chen, L. Tang, W. Huo, X. Huang, Q. Cao, Genetically programmable vesicles for enhancing CAR-T therapy against solid tumors, Adv. Mater. (2023) e2211138 (Deerfield Beach, Fla.) n/a(n/a).
[30] W. Hu, Z. Zi, Y. Jin, G. Li, K. Shao, Q. Cai, X. Ma, F. Wei, CRISPR/Cas9-mediated PD-1 disruption enhances human mesothelin-targeted CAR T cell effector functions, Cancer Immunol. Immunother. (2018).
[31] M. Hao, S. Hou, W. Li, K. Li, L. Xue, Q. Hu, L. Zhu, Y. Chen, H. Sun, C. Ju, C. Zhang, Combination of metabolic intervention and T cell therapy enhances solid tumor immunotherapy, Sci. Transl. Med. 12 (571) (2020).
[32] X. Li, N. Gong, F. Tian, S. Zhang, Y. Zhang, Y. Wang, G. Qing, Y. Wang, F. Li, Y. Xu, L. Zhang, J. Wang, Q. Ni, Y. Gan, C. Gu, H. Jiang, X. Huang, X. Shi, T. Zhang, Y. Wu, X.-J. Liang, Suppression of cytokine release syndrome during CAR-T-cell therapy via a subcutaneously injected interleukin-6-adsorbing hydrogel, Nat. Biomed. Eng. 7 (9) (2023) 1129–1141.
[33] S.J. Priceman, D. Tilakawardane, B. Jeang, B. Aguilar, J.P. Murad, A.K. Park, W. C. Chang, J.R. Ostberg, J. Neman, R. Jandial, J. Portnow, S.J. Forman, C.E. Brown, Regional delivery of chimeric antigen receptor-engineered T cells effectively targets HER2(+) breast cancer metastasis to the brain, Clin. Cancer Res.: Off. J. American Assoc. Cancer Res. 24 (1) (2018) 95–105.
[34] S. Modi, C. Saura, T. Yamashita, Y.H. Park, S.B. Kim, K. Tamura, F. Andre, H. Iwata, Y. Ito, J. Tsurutani, J. Sohn, N. Denduluri, C. Perrin, K. Aogi, E. Tokunaga, S.A. Im, K.S. Lee, S.A. Hurvitz, J. Cortes, C. Lee, S. Chen, L. Zhang, J. Shahidi, A. Yver, I. Krop, Trastuzumab deruxtecan in previously treated HER2-positive breast cancer, N. Engl. J. Med. 382 (7) (2020) 610–621.
[35] X. Liu, S. Jiang, C. Fang, S. Yang, D. Olalere, E.C. Pequignot, A.P. Cogdill, N. Li, M. Ramones, B. Granda, L. Zhou, A. Loew, R.M. Young, C.H. June, Y. Zhao, Affinity-tuned ErbB2 or EGFR chimeric antigen receptor T cells exhibit an increased therapeutic index against tumors in mice, Cancer Res. 75 (17) (2015) 3596–3607.
[36] Y. Yuan, S. Zhou, C. Li, X. Zhang, H. Mao, W. Chen, X. Jiang, Cascade downregulation of the HER family by a dual-targeted recombinant protein-drug conjugate to inhibit tumor growth and metastasis, Adv. Mater. 34 (23) (2022) e2201558.
[37] D.V. Foss, J.J. Muldoon, D.N. Nguyen, D. Carr, S.U. Sahu, J.M. Hunsinger, S. K. Wyman, N. Krishnappa, R. Mendonsa, E.V. Schanzer, B.R. Shy, V.S. Vykunta, V. Allain, Z. Li, A. Marson, J. Eyquem, R.C. Wilson, Peptide-mediated delivery of CRISPR enzymes for the efficient editing of primary human lymphocytes, Nat. Biomed. Eng. 7 (5) (2023) 647–660.
[38] M. Black, A. Trent, Y. Kostenko, J.S. Lee, C. Olive, M. Tirrell, Self-assembled peptide amphiphile micelles containing a cytotoxic T-cell epitope promote a protective immune response in vivo, Adv. Mater. 24 (28) (2012) 3845–3849.
[39] T.T. Smith, H.F. Moffett, S.B. Stephan, C.F. Opel, A.G. Dumigan, X. Jiang, V. G. Pillarisetty, S.P.S. Pillai, K.D. Wittrup, M.T. Stephan, Biopolymers codelivering engineered T cells and STING agonists can eliminate heterogeneous tumors, J. Clin. Invest. 127 (6) (2017) 2176–2191.
[40] S.C. Katz, G.R. Point, M. Cunetta, M. Thorn, P. Guha, N.J. Espat, C. Boutros, N. Hanna, R.P. Junghans, Regional CAR-T cell infusions for peritoneal carcinomatosis are superior to systemic delivery, Cancer Gene Ther. 23 (5) (2016) 142–148.
[41] P. Agarwalla, E.A. Ogunnaike, S. Ahn, K.A. Froehlich, A. Jansson, F.S. Ligler, G. Dotti, Y. Brudno, Bioinstructive implantable scaffolds for rapid in vivo manufacture and release of CAR-T cells, Nat. Biotechnol. 40 (8) (2022) 1250–1258.
[42] P.S. Adusumilli, L. Cherkassky, J. Villena-Vargas, C. Colovos, E. Servais, J. Plotkin, D.R. Jones, M. Sadelain, Regional delivery of mesothelin-targeted CAR T cell therapy generates potent and long-lasting CD4-dependent tumor immunity, Sci. Transl. Med. 6 (261) (2014) 261ra151.
[43] S.B. Stephan, A.M. Taber, I. Jileaeva, E.P. Pegues, C.L. Sentman, M.T. Stephan, Biopolymer implants enhance the efficacy of adoptive T-cell therapy, Nat. Biotechnol. 33 (1) (2015) 97–101.
[44] W. Zhou, S. Lei, M. Liu, D. Li, Y. Huang, X. Hu, J. Yang, J. Li, M. Fu, M. Zhang, F. Wang, J. Li, K. Men, W. Wang, Injectable and photocurable CAR-T cell formulation enhances the anti-tumor activity to melanoma in mice, Biomaterials 291 (2022) 121872.
[45] H. Jiang, Q. Wang, L. Li, Q. Zeng, H. Li, T. Gong, Z. Zhang, X. Sun, Turning the old adjuvant from gel to nanoparticles to amplify CD8(+) T cell responses, Adv. Sci. 5 (1) (2018) 1700426.
[46] P. Yang, Y. Peng, Y. Feng, Z. Xu, P. Feng, J. Cao, Y. Chen, X. Chen, X. Cao, Y. Yang, J. Jie, Immune cell-derived extracellular vesicles – new strategies in cancer immunotherapy, Front. Immunol. 12 (5259) (2021) 771551.
[47] L. Chen, Y. Xiong, Y. Hu, C. Yu, G. Liu, Regulatory T cell-exosomal miR-142-3p promotes angiogenesis and osteogenesis via TGFBR1/SMAD2 inhibition to accelerate fracture repair, Chem. Eng. J. 427 (119552) (2022) 131419.
[48] M. Koneru, T.J. Purdon, D. Spriggs, S. Koneru, R.J. Brentjens, IL-12 secreting tumor-targeted chimeric antigen receptor T cells eradicate ovarian tumors in vivo, OncoImmunology 4 (3) (2015) e994446.
[49] J. Lötscher, I.L.A.A. Martí, N. Kirchhammer, E. Cribioli, G.M.P. Giordano Attianese, M.P. Trefny, M. Lenz, S.I. Rothschild, P. Strati, M. Künzli, C. Lotter, S.H. Schenk, P. Dehio, J. Löliger, L. Litzler, D. Schreiner, V. Koch, N. Page, D. Lee, J. Grählert, D. Kuzmin, A.V. Burgener, D. Merkler, M. Pless, M.L. Balmer, W. Reith, J. Huwyler, M. Irving, C.G. King, A. Zippelius, C. Hess, Magnesium sensing via LFA-1 regulates CD8(+) T cell effector function, Cell 185 (4) (2022) 585–602.e29.